INTERNATIONAL JOURNAL OF OPTIMIZATION IN CIVIL ENGINEERING
Int. J. Optim. Civil Eng., 2016; 6(3):405-422

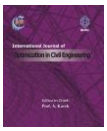

ISOGEOMETRIC TOPOLOGY OPTIMIZATION OF STRUCTURES USING LEVEL SET METHOD INCORPORATING SENSITIVITY ANALYSIS

M. Roodsarabi, M. Khatibinia[*, †] and S.R. Sarafrazi
Department of Civil Engineering, University of Birjand, Birjand, Iran

ABSTRACT

This study focuses on the topology optimization of structures using a hybrid of level set method (LSM) incorporating sensitivity analysis and isogeometric analysis (IGA). First, the topology optimization problem is formulated using the LSM based on the shape gradient. The shape gradient easily handles boundary propagation with topological changes. In the LSM, the topological gradient method as sensitivity analysis is also utilized to precisely design new holes in the interior domain. The hybrid of these gradients can yield an efficient algorithm which has more flexibility in changing topology of structure and escape from local optimal in the optimization process. Finally, instead of the conventional finite element method (FEM) a Non–Uniform Rational B–Splines (NURBS)–based IGA is applied to describe the field variables as the geometry of the domain. In IGA approach, control points play the same role with nodes in FEM, and B–Spline functions are utilized as shape functions of FEM for analysis of structure. To demonstrate the performance of the proposed method, three benchmark examples widely used in topology optimization are presented. Numerical results show that the proposed method outperform other LSMs.

Keywords: topology optimization; isogeometric analysis; level set method; sensitivity analysis; Non–Uniform Rational B–Splines.

Received: 10 November 2015; Accepted: 2 February 2016

1. INTRODUCTION

In the past three decades, topology optimization has been considered as a powerful and popular tool for designers and engineers [1]. Furthermore, topology optimization has been extensively utilized to a variety of structural optimization problems such as the stiffness

[*]Corresponding author: Department of Civil Engineering, University of Birjand, Birjand, Iran
[†]E-mail address: m.khatibinia@birjand.ac.ir (M. Khatibinia)

maximization problem, vibration problems, optimum design problems for compliant mechanisms, and thermal problems. The main aim of topology optimization is to find the geometry of a design in terms of shape and topology to perform a specific task optimally, ranging from discrete gridlike structures to continuum structures [2, 3]. In contrast to the detailed designs (e.g. size and shape optimizations) of a structure, topology optimization does not require a close–to–optimal initial design and is able to generate optimal geometries when intuitive design approaches fail, e.g., due to complex interdependencies between design parameters and the structural response. A number of methods such as Optimality Criteria (OC) methods [4, 5], the approximation methods [6–9], the Method of Moving Asymptotes (MMA) [9–11], Evolutionary Structural Optimization (ESO) method [12] and even more heuristic methods such as genetic algorithm [13] and ant colony [14] have been proposed for solving the topology optimization problems.

Recently, the level set method (LSM) originally proposed by Osher and Sethian [15] has been applied as a new technique well suited to optimizing shape and topology of structures. The LSM is firstly introduced for the structural topology optimization by Sethian and Wiegmann [16]. In the LSMs, the boundary is implicitly represented as the zero level–set of a higher dimensional level set function of Lipschitz continuity. The level set function is defined over a fixed reference domain that includes all the admissible shapes and topologies of the design domain. In the LSMs, a pseudo–time is normally defined into the level set function to enable the dynamic evolution of the discrete level set function [17, 18]. A level set equation called the Hamilton–Jacobi Partially Differential Equation (H–J PDE) is utilized to describe the level set representation of dynamic implicit surfaces. Appropriate numerical approachs [15] are proposed to obtain the steady–state solution of the H–J PDE. The motion of the level set function along the normal direction can lead to the motion of the design boundary, as well as the shape and topological changes of the structure at the zero level–set. In the shape and topology optimization process based on the LSM approach, the geometry and shape changes are described as propagation of the boundary with a given speed function only defined at the interface. However, due to the mass conservative law, the LSM cannot create new holes inside the solid domain [16]. This drawback is considerably increased in topology optimization process. Hence, the topological gradient method as sensitivity analysis was proposed to overcome this drawback [17]. It has been indicated that this approach efficiently create new holes such that the strong dependency of the optimal topology on the initial design can be alleviated. In recent years, studies on structural topology optimization based on the LSMs have been presented [18–20].

In the development of advanced computational methodologies, Hughes et al. [21] proposed a Non–Uniform Rational B–Splines (NURBS)–based isogeometric analysis (IGA) to eliminate the gap between computer–aided design (CAD) and finite element analysis. In contrast to the standard finite element method (FEM) with Lagrange polynomial basis, the IGA approach utilizes more general basis functions such as NURBS that are common in CAD approaches. Thus, IGA is very promising because it can directly use CAD data to describe both exact geometry and approximate solution.

The main contribution of the present study is to introduce a hybrid of the LSM incorporating sensitivity analysis and IGA for topology optimization of structures. To achieve this purpose, first, the LSM based on the shape gradient is utilized to solve the topology optimization problem. The topological gradient method is also incorporated in the

LSM process to precisely design new holes in the interior domain. Then, instead of the conventional FEM a NURBS–based IGA is applied to describe the field variables as the geometry of the domain. In IGA approach, control points is considered as the same role with nodes in FEM and B–Spline basis functions are utilized as shape functions of FEM for analysis of structure. Three benchmark examples are presented to demonstrate the validity of the proposed method. The optimum results are compared with those reported in the literature. The optimal results reveal that the proposed method is a powerful topology optimization algorithm with fast convergence rate in comparison with the other LSMs.

2. STRUCTURAL TOPOLOGY OPTIMZATION PROBLEM

In this study, a linear elastic structure is considered to describe the problem of structural optimization. For this perpose, $\Omega \subseteq \boldsymbol{R}^n$ is assumed an open and bounded set occupied by a linear isotropic elastic structure. The boundary of Ω consists of three parts $\Gamma = \partial\Omega = \Gamma_d \cup \Gamma_u \cup \Gamma_t$, with Dirichlet boundary conditions on Γ_u and Neumann boundary conditions on Γ_t. Furthermore, Γ_d is traction free. The displacement field in Ω is the unique solution of the linear elastic system and is expressed as [22]:

$$\begin{cases} -div\,\sigma(u) = p & \text{in } \Omega \\ u = u_0 & \text{in } \Gamma_u \\ \sigma(u).N = \tau & \text{in } \Gamma_t \end{cases} \tag{1}$$

where u is the nodal displacement field function. The strain tensor ε and the stress tensor σ at any point Ω are defined in the usual form as:

$$\begin{cases} \sigma_{ij}(u) = E_{ijkl}\,\varepsilon_{kl}(u) \\ \varepsilon_{ij}(u) = \dfrac{1}{2}\left(\dfrac{\partial u_i}{\partial x_j} + \dfrac{\partial u_j}{\partial x_i}\right) \end{cases} \tag{2}$$

where E_{ijkl} is the elasticity tensor; and ε_{ij} is the liberalized strain tensor. The topology optimization is to find a suitable shape in the admissible design space, so that the objective functional can reach its minimum or at least a local minimum. Therefore, this can be expressed as follows [23, 24]:

$$\begin{aligned} &\text{Minimize}: \quad J(u) = \int_\Omega F(u)\,d\Omega \\ &\text{Subject to}: \quad \int_\Omega E_{ijkl}\,\varepsilon_{ij}(u)\,\varepsilon_{kl}(v)\,d\Omega = \int_\Omega p\,v\,d\Omega + \int_{\Gamma_t} \tau\,v\,d\Gamma \quad \text{for all} \quad v \in U \\ &\qquad\qquad u = u_0 \quad \text{on} \quad \Gamma_u \\ &\qquad\qquad Vol = \int_\Omega d\Omega \le V_{\max} \end{aligned} \tag{3}$$

where v is the adjoint displacement field function in the space U of kinematically admissible displacement fields. Field function u_0 prescribes displacement field on partial boundary Γ_u. p is the body force. τ is the boundary traction. The inequality describes the limit on the amount of material in terms of the maximum admissible volume $V_{\max}$ of the design domain.

3. IMPLICIT REPERESENTION OF THE BOUNDARY

Level set method (LSM) is a high effective method developed by Osher and Sethian [15] may also be referred to as implicit moving boundary models. The boundary $\partial\Omega$ is implicitly defined as an iso–surface of the embedding $\phi(x)$ as shown in Fig. 1.

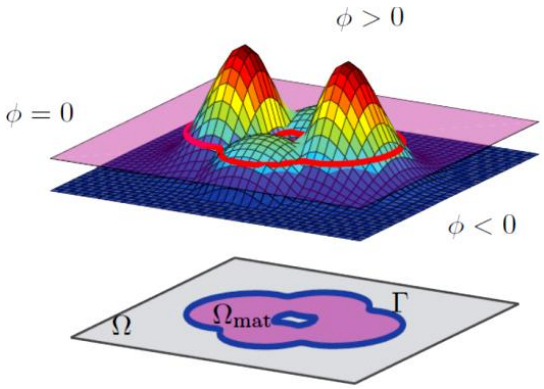

Figure 1. Diagram of level set function and its implicit boundary

These definitions are also expressed as follows [15, 24]:

$$\begin{cases} \phi(x) < 0 \ : \ \forall \ x \in \Omega / \bar{\Omega} \\ \phi(x) = 0 : \forall \ x \in \partial\Omega \\ \phi(x) > 0 \ : \forall \ x \in \Omega \setminus \partial\Omega \end{cases} \tag{4}$$

The implicit function $\phi(x)$ is used to represent the boundary and to optimize it, as it was originally developed for curve and surface evolution. The change of the implicit function $\phi(x)$ is governed by the simple convection equation as:

$$\frac{\partial\phi(x,t)}{\partial t} + \nabla\phi(x,t).V(x) = 0 \tag{5}$$

where $V(x)$ defines the velocity of each point on the boundary. The parameter t is a fictitious time parameter that represents the optimization iteration number, and the time step, t, is chosen in such away that the Courant–Friedrichs–Lewy (CFL) conditionis satisfied [17]. Since the tangential components of V would vanish, it can be written as:

$$\frac{\partial \phi(x,t)}{\partial t} = V_N \left|\nabla \phi(x,t)\right| \tag{6}$$

The normal velocity V_N is related to the sensitivity of the shape to the boundary variation. These two H–J PDEs are the well–known level set equations [17, 22]. To ensure the convergence of the differential equation (5) using finite differences, the step time should satisfy CFL [17] condition:

$$\Delta t \le \frac{h}{\max\left|V_n\right|} \tag{7}$$

where h is the minimum distance between points of the grid and max $\left|V_n\right|$ is the maximum value of the points of the grid.

Based on the level set theory, the topology optimization problem is transformedinto a problem of finding the steady–state solution of the H–J equation. As it can bee seen from Equations (6) and (7), after the initial level set function $\phi(x)$ is identified, to get afeasible steady–state solution, the crux is to find a meaningful velocity field. Hence, the optimization problem can be formulated using the LSM, as:

$$\begin{aligned} &\text{Minimize}: \ J(u,\phi) = \int_\Omega F(u) H(\phi) d\Omega \\ &\text{subject to}: \\ &\qquad a(u,v,\phi) = L(v,\phi), u\,|_{\partial D_u} \ , \ \forall v \in U \\ &\qquad Vol = \int_\Omega H(\phi) d\Omega - V_{\max} \le 0 \end{aligned} \tag{8}$$

where $a(u,v,\phi)$ and $L(v,\phi)$ are the energy bilinear form and the load linear form, respectively. The terms are given as follows:

$$\begin{aligned} a(u,v,\phi) &= \int_\Omega E_{ijkl}\, \varepsilon_{ij}(u) \varepsilon_{kl}(v) H(\phi) d\Omega \\ L(v,\phi) &= \int_\Omega p\, v H(\phi) d\Omega + \int_\Omega v \tau \delta(\phi) \left|\nabla \phi\right| d\Omega \end{aligned} \tag{9}$$

where $\delta(x)$ and $H(x)$ are the Dirac function and the Heaviside function, recpectivily.

3. OPTIMIZATION METHOD WITH SHAPE SENSITIVITY

To find a minimization solution to the optimization problem, it is needed to find the variation of the objective functional with respect to a variation of the design variable. This process is usually called sensitivity analysis. And, since in this case the design variable is the shape represented by the LSM, it is also called shape sensitivity analysis and the result is

called shape gradient or shape derivative. Based on the shape gradient analysis, the steepest descent direction is directly obtained by:

$$V_n = \left(F(u) + p.v - div(\tau v) - E\varepsilon(u) : \varepsilon(v)\right) \tag{10}$$

Thus, this choice would give a computational framework for obtaining an approximate solution such as the algorithms used in [24, 25].

4. OPTIMIZATION METHOD WITH TOPOLOGICAL SENSITIVITY

4.1 Topological gradient

Topological gradient as sensitivity measure has been used by many researchers to solve topology optimization problems [17, 26–28]. This method can account for the sensitivity of creating a hole at the interior point of the design domain. Topological gradient is defined by several ways. The definition proposed by Sokolowski and Zochowski [26] is as follows:

$$TD(x) = \lim_{|\omega|\to 0} \frac{J\left(S \setminus \bar{\omega}_\varepsilon(x)\right) - J(s)}{\left|\bar{\omega}_\varepsilon(x)\right|} \tag{11}$$

where S denotes the design domain, ω represents a small hole centered at $x \in S$ and of radius εa. J is the objective functional of interest. $|\omega|$ is the measure of ω. Thus, $\left|\bar{\omega}_\varepsilon(x)\right| = \pi \varepsilon^2 a^2$.

4.2 The topological gradient concept with volume constraint

In order to solve the optimization problem (3), the augmented Lagrangian method is utilized. Hence, the following definition is the object function of the optimization problem with volume constrain:

$$J'(u,\phi) = \int_\Omega F(u) H(\phi) d\Omega + \lambda\left(Vol - V_{\max}\right) \tag{12}$$

or

$$J'(u,\phi) = J(u,\phi) + \lambda\left(V - V_{\max}\right) \tag{13}$$

where λ is the Lagrange multiplier. Then, the topological gradient with volume constraint is:

$$TD'(x) = \lim_{|\omega|\to 0} \frac{J'\left(S \setminus \bar{\omega}_\varepsilon(x)\right) - J'(s)}{\left|\bar{\omega}_\varepsilon(x)\right|} \tag{14}$$

by substituting (13) into (14), it is obtained:

$$TD'(x) = TD - \lambda \tag{15}$$

where λ can be determined with [25]:

$$\lambda = -\frac{\int_{\partial\Omega} \beta(u, w, \phi)\, d\Gamma}{\int_{\partial\Omega} d\Gamma} \tag{16}$$

where $\beta(u, w, \phi)$ describes the sensitivity of the objective function $J(u, \phi)$ with respect to the boundary variation of the design. Although, the value of TD is always greater than zero, when the value of λ is great than TD, the value of TD will be less than zero. That's mean the hole can be created to decrease the object function.

5. ISOGEOMETRIC ANALYSIS

Isogeometric analysis (IGA) has developed as powerful computational approach that offers the possibility of integrating finite element analysis (FEA) into conventional NURBS–based CAD tools [21]. The concept of the IGA is great interest in various engineering problems that is utilized for the discretization of partial differential equations. The main advantage of IGA is to utilize the NURBS basis functions that accurately model the exact geometries of solution space for numerical simulations of physical phenomena.

5.1 B–Spline and NURBS basis function

A NURBS surface is parametrically constructed as [29]:

$$S(\xi, \eta) = \frac{\sum_{i=1}^{n} \sum_{j=1}^{m} N_{i,p}(\xi) N_{j,q}(\eta) \omega_{i,j} P_{i,j}}{\sum_{i=1}^{n} \sum_{j=1}^{m} N_{i,p}(\xi) N_{j,q}(\eta) \omega_{i,j}} \tag{17}$$

where $P_{i,j}$ are (n, m) control points, $\omega_{i,j}$ are the associated weights and $N_{i,p}(\xi)$ and $N_{j,q}(\eta)$ are the normalized B–splines basis functions of degree p and q respectively. The i th B–splinebasis function of degree p, denoted by $N_{i,p}(\xi)$, is defined recursively as:

$$N_{i,0}(\xi) = \begin{cases} 1 & \text{if} \quad \xi_i \le \xi < \xi_{i+1} \\ 0 & \text{otherwise} \end{cases} \tag{18}$$

and

$$N_{i,p}(\xi)=\frac{\xi-\xi_i}{\xi_{i+p}-\xi_i}N_{i,p-1}(\xi)+\frac{\xi_{i+p+1}-\xi}{\xi_{i+p+1}-\xi_{i+1}}N_{i+1,p-1}(\xi) \tag{19}$$

where $\xi=\{\xi_0,\xi_1,.....\xi_r\}$ is the knot vector and, ξ_i are a non–decreasing sequence of realnumbers, which are called knots. The knot vector $\eta=\{\eta_0,\eta_1,...,\eta_s\}$ is employed to define the $N_{j,q}(\eta)$ basis functions for other direction. The interval $[\xi_0,\xi_r]\times[\eta_0,\eta_s]$ forms a patch [21]. A knot vector, for instance in ξ direction, is called open if the first and last knots have a multiplicity of $p+1$. In this case, the number of knots is equal to $r=n+p$. Also, the interval $[\xi_i,\xi_{i+1})$ is called a knot span where at most $p+1$ of the basis functions $N_{i,p}(\xi)$ are non–zero which are $N_{i-p,p}(\xi),....,N_{i,p}(\xi)$.

5.2 NURBS based isogeometric analysis formulation

By using the NURBS basis functions for a patch p, the approximated displacement functions $u^p=[u,v]$ can be expressed as [11]:

$$u^p(\xi,\eta)=\sum_{i=1}^{n}\sum_{j=1}^{m}R_{i,j}(\xi,\eta)u_{i,j}^p \tag{20}$$

where $R_{i,j}(\xi,\eta)$ is the rational term in Equation (17). Furthermore, the geometry is approximated by B–spline basis functions as [11]:

$$S^p(\xi,\eta)=\sum_{i=1}^{n}\sum_{j=1}^{m}R_{i,j}(\xi,\eta)S_{i,j}^p \tag{21}$$

By using the local support property of NURBS basis functions, Equations (20) and (21) can be summarized as it follows in any given $(\xi,\eta)\in[\xi_i,\xi_{i+1})\times[\eta_j,\eta_{j+1})$.

$$u^p(\xi,\eta)=\left(u^p(\xi,\eta),v^p(\xi,\eta)\right)=\sum_{k=i-p}^{i}\sum_{l=j-q}^{j}R_{k,l}(\xi,\eta)U_{k,l}^p=\boldsymbol{RU} \tag{22}$$

$$S^p(\xi,\eta)=\left(x^p(\xi,\eta),y^p(\xi,\eta)\right)=\sum_{k=i-p}^{i}\sum_{l=j-q}^{j}R_{k,l}(\xi,\eta)P_{k,l}^p=\boldsymbol{RP} \tag{23}$$

Final, the stiffness matrix for a single patch is also computed as,

$$\mathbf{K}=\iint_{\Omega}\mathbf{B}^T(\xi,\eta)\mathbf{D}\mathbf{B}(\xi,\eta)\left|\mathbf{J}\right|\bar{t}\,d\xi\,d\eta \tag{24}$$

where $\bar{t}$ is the thickness, $\mathbf{B}(\xi,\eta)$ is the strain–displacement matrix, and **J** is the jacobian matrix which maps the parametric space to the physical space. **D** is the elastic material property matrix for plane stress. It is noted that in this study the standard Gauss–quadrature over each knot space is utilized for numerical integration.

6. LEVEL SET BASED ISOGEOMETRIC TOPOLOGY OPTIMIZATION

In order to implement isogeometric topology optimization based on the LSM incorporating sensitivity analysis, the NURBS based–IGA approach is utilized instead of in the conventional FEM. In fact, in IGA control points play the same role with nodes in FEM and B–Spline basis functions are utilized as shape functions of FEM for analysis of structure. Boundary conditions are directly imposed on control points. Numerical integration is implemented almost same with FEM in order to transform the parametric domain to master element for Gauss quadrature. The design model are also modeled using a fixed isogeometric. For achieving this purpose, the "Ersatz material" approach [17] is utilized in this study in order to avoid the time–consuming re–meshing process of design model topology optimization procedure. Based on the "Ersatz material" approach, the elements associated with the void (hole) region are modeled by a weak material. Therefore, the flowchart of discretized isogeometric topology optimization method based on the LSM is depicted in Fig. 2.

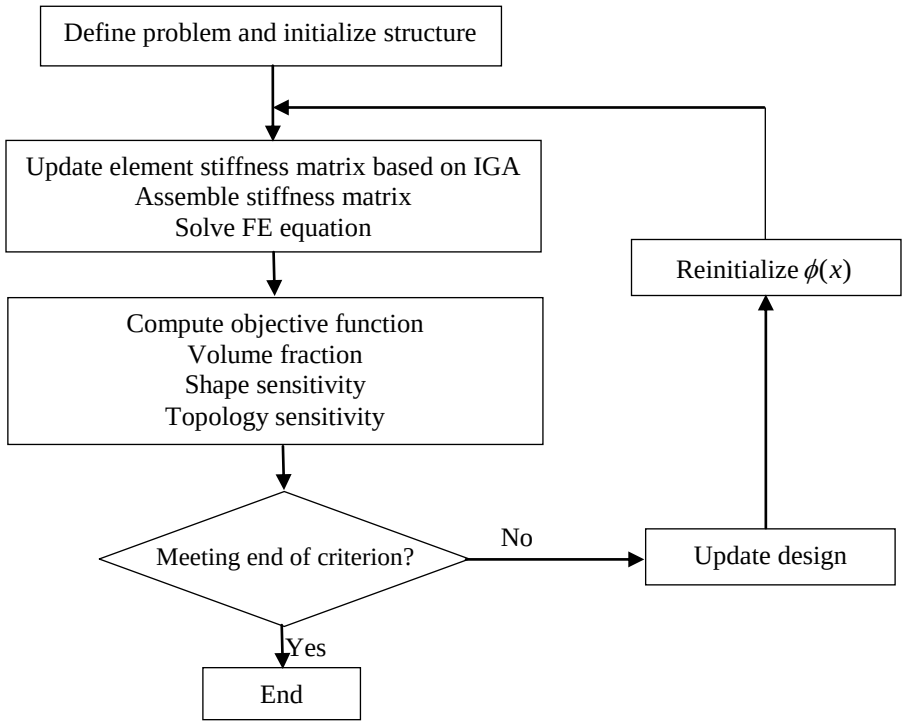

Figure 2. Flowchart of the isogeometric topology optimization based on the LSM incorporating the sensitivity analysis

7. NUMERICAL EXAMPLE

To demonstrate the isogeometric topology optimization of structures using the LSM incorporating the sensitivity analysis, three examples of isotropic plane elasticity problem are presented in this section. In all examples the modulus of elasticity, the Poisson's ratio

and thickness are considered as $1Pa$, 0.3 and $0.01m$, respectively. In the analysis procedure of structures, "Ersatz material" approach [17] is utilized, which fills the void areas with one weak material. For this purpose, Young's modulus of Ersatz material is assumed as $10^{-3}Pa$. The order of NURBS basis functions in each direction is equal to be 2.

7.1 Cantilever beam

The first problem is the cantilever beam shown in Fig. 3, which is a benchmark problem in topology optimization. As shown in Fig. 3, the length of the domain is $L=80mm$ and the height is $H=40mm$. The cantiliver is subjected to a concentrated load P=1N at the middle point of the free end. The volume constraint is 40% of the total domain volume. The time step, t, is taken as 10; and the coefficient of the topology gradient is taken as 2.

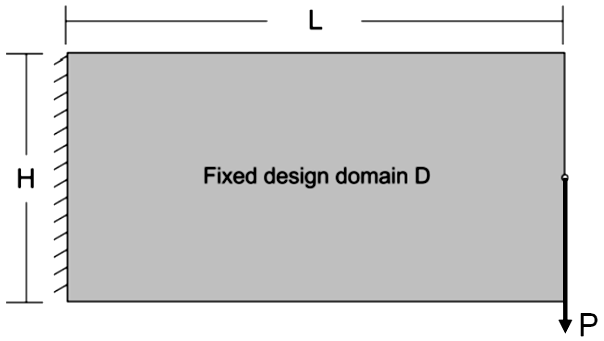

Figure 3. Fixed design domain and boundary condition of a cantilever example

In this example, the initial geometry is modeled based on a bi–quadratic NURBS geometry with 10×6 control points. The open knot vectors are respectively {0, 0, 0, 0.125, 0.25, 0.375, 0.5, 0.625, 0.75, 0.875, 1, 1, 1} and {0, 0, 0, 0.25, 0.5, 0.75, 1, 1, 1} in ξ and η direction, thus leading to 8×4 knot spans. By subdividing each knot span into 10 equal parts in ξ and η direction, the physical mesh with 80×40 knot spans and the control mesh with 82×42 control points are obtained. The evolution procedure of structural topology based on the proposed method is shown from Figs. 4(a) to 4(f). The final topology of the cantilever is also depicted in Fig. 4(f).

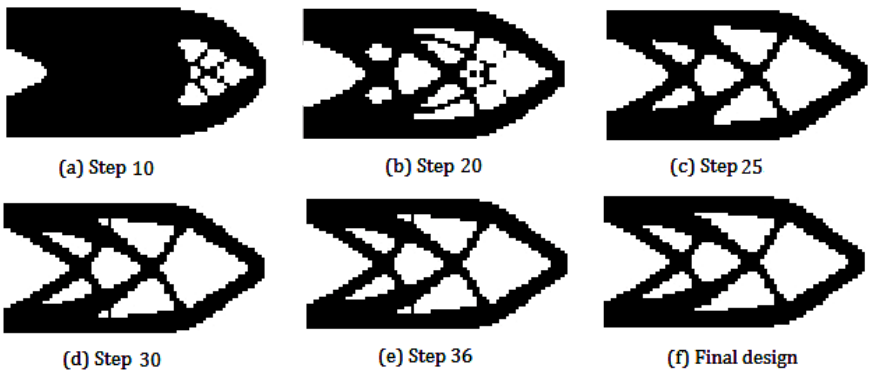

Figure 4. The evolution of optimal topology of the cantilever beam

In recent years, this example has investigated by other researchers [18, 19, 31]. The final optimal topology obtained the proposed method of this study is compared with those obtained in other studies [18, 19, 31] and shown in Fig. 5.

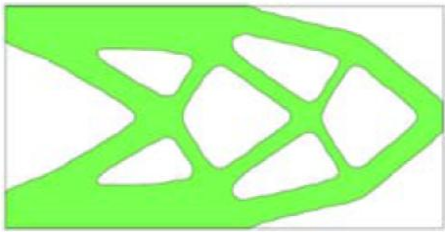

(a) The conventional LSM with FEM [18]

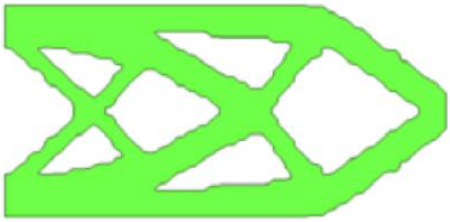

(b) The binary LSM and holes with FEM [18]

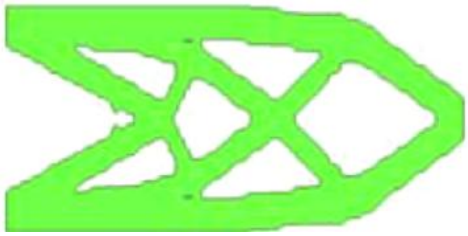

(c) The binary LSM and non-holes with FEM [18]

(d) The radial basis function LSM with IGA [19]

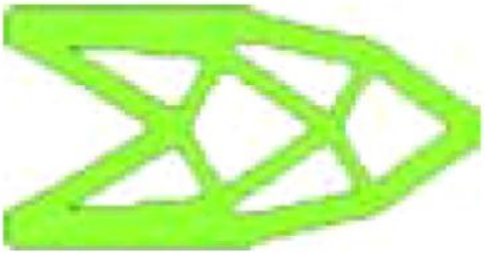

(e) The enhanced LSM with FEM [31]

(f) This study

Figure 5. The comparison of the final optimal topology in this study with the other studies

As can been seen from Fig. 5, the final design obtained in this study is similar to those reported in the literature. Furthermore, the optimal results of this study and other studies are compared and presented in Table 1.

Table 1: Comparison of the proposed method and other studies

Schemes	Objective function ($J(\Omega)$)	Number of convergence Iterations
The conventional LSM with FEM [18]	63.88	200
The binary LSM and holes with FEM [18]	62.73	115
The binary LSM and non-holes with FEM [18]	64.18	100
The radial basis function LSM with IGA [19]	62.66	60
The enhanced LSM with FEM [31]	80.22	81
The proposed method	62.082	37

It is obvious from Table 1 that the performance of the proposed algorithm is more efficient than the other LSMs. The evolution of the compliance and the volume fraction are shown in Fig. 6. The value of the compliance at the optimal design is 62.082.

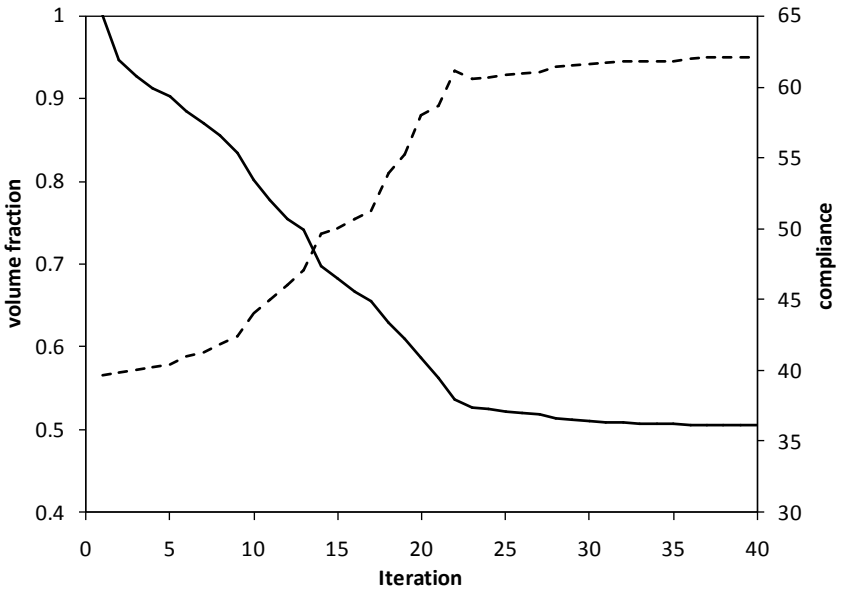

Figure 6. The convergence histories of the compliance and volume ratio

7.2 Messerschmitt–Bölkow–Blom beam

Messerschmitt–Bölkow–Blom (MBB) beam considered as the second example is the benchmark problem for topology optimization. The geometry model and loading conditions of the MBB beam is shown in Fig. 7. The length of the domain is $L = 120mm$ and the height is $H = 30mm$. The problem is subjected to a concentrated load P=1*N* at the upper half of the vane. In the optimization procedure, the specified material volume fraction is 40%.

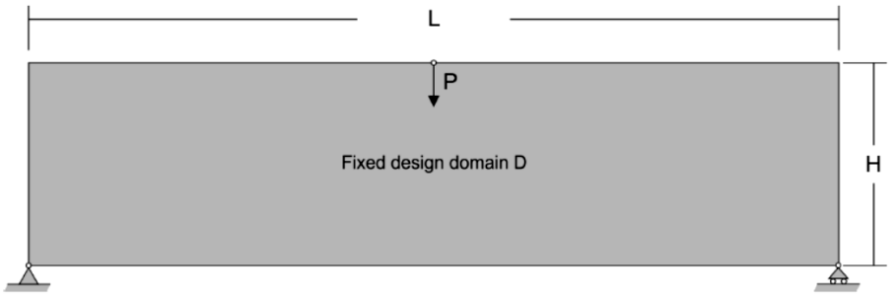

Figure 7. Fixed design domain and boundary condition of the MBB beam

In the first stage, the topology optimization is performed based on the proposed method with 120×30 mesh isogeometric and the topology evolving history is depicted in Fig. 8. The topology evolving history shows that the final topology is obtained in the 51 iterations.

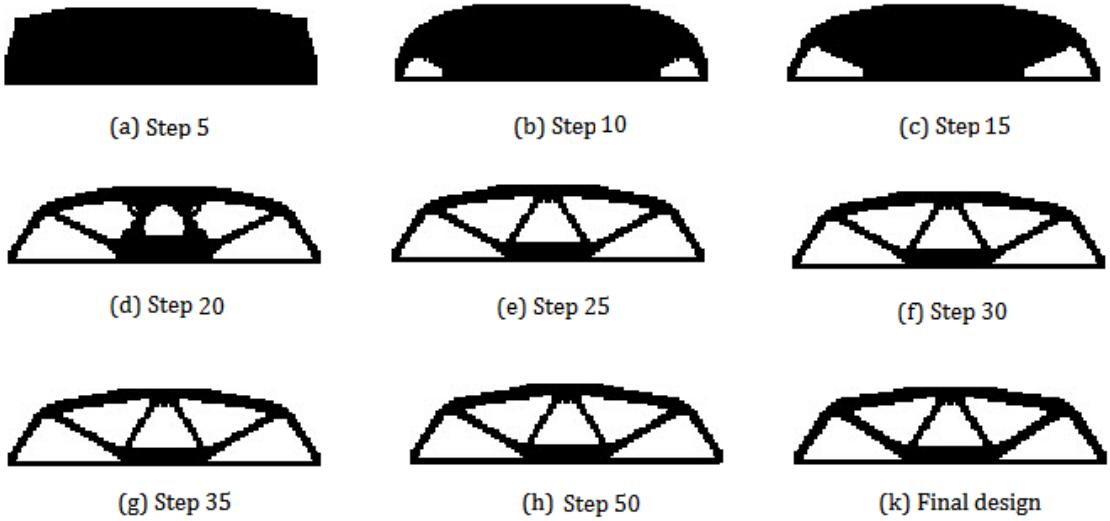

Figure 8. The evolution of optimal topology of the MBB beam

In second stage, FEM as an analyzer instead of IGA is utilized in order to demonstrate the performance of the proposed method. The number of degree of freedoms in FEM are also equal to those of IGA. The final topology optimization obtained the proposed method is compared with that obtained by the LSM incorporating sensitivity analysis and FEM and shown in Fig. 9.

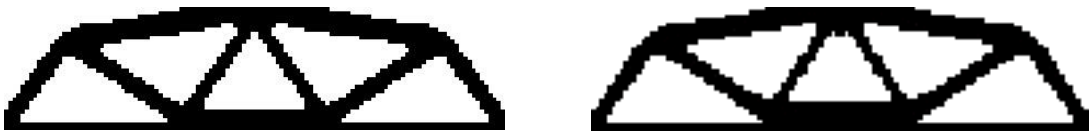

(a) (b)

Figure 9. The comparison of the final optimal topology based on (a) FEM and (b) IGA

It can been observed from Fig. 9 that the final design obtained in the IGA is similar to that of FEM. The optimal results obtained with the two different schemes are listed in Table 2.

Table 2: Comparison of the results obtained based on the FEA and IGA

Schemes	Objective function ($J(\Omega)$)	Number of convergence Iterations
FEM	48.220	72
IGA	48.156	48

The results of Table 2 indicates that the IGA outperformed the FEM. Figs. 10 and 11 show the structural strain energy variation history during optimization for the IGA and the FEM, respectively. In thses figures the iteration history of material usage within the design domain during topology evolving are also depicted.

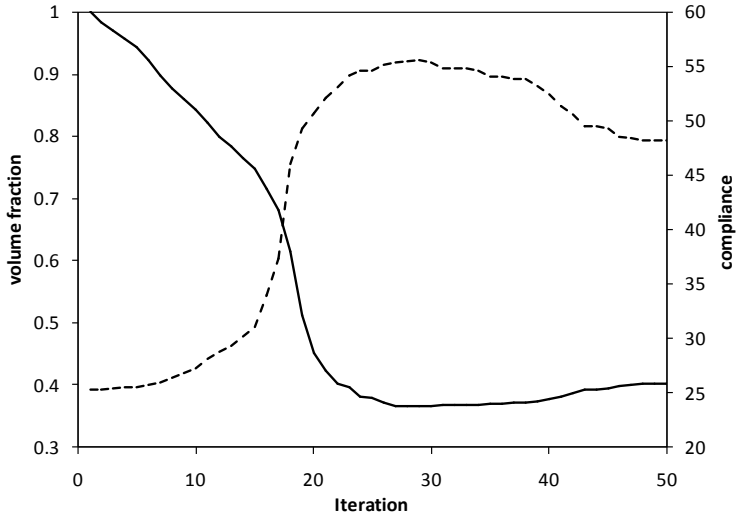

Figure 10. The convergence histories of the compliance and volume ratio for the IGA

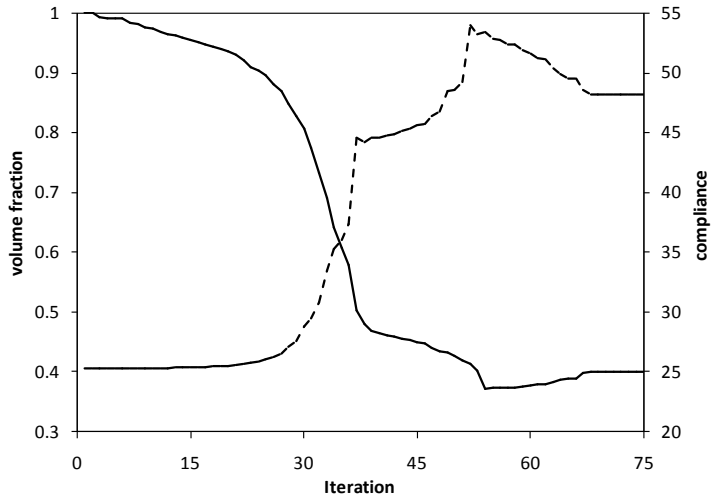

Figure 11. The convergence histories of the compliance and volume ratio for the FEM

It can be can be concluded from Figs. 10 and 11 that the convergence of the IGA is faster than that of the FEM. The optimal design generated by using the proposed method is also compared with that reported in Mohamadian and Shojaee [32] and shown in Fig. 12.

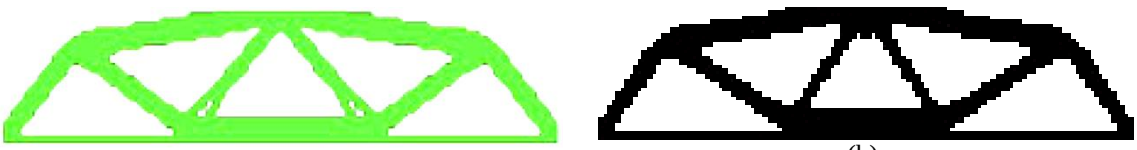

(a) (b)

Figure 12. The comparison of the final optimal topology based on (a) the binary LSM and FEM, (b) the proposed method

As it is observed the obtained topologies are basically the same. However, it is noticed that the corners of the diagonal members are different.

7.3 Michell structure

The third problem is the Michell structure shown in Fig. 13. The length of the domain is $L = 80mm$ and the height is $H = 40mm$. the problem is subjected to a concentrated load $P = 1N$ at the bottom half of the vane. In the optimization procedure, the specified material volume fraction is 40%.

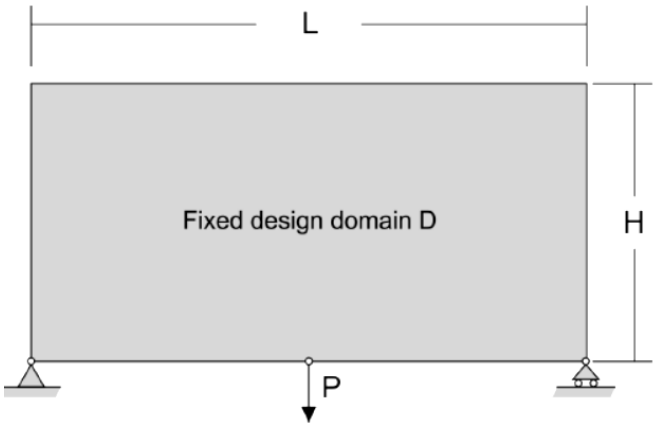

Figure 13. Fixed design domain and boundary condition of the Michell–type structure

In the first stage, the topology optimization is performed based on the proposed method with 80×40 mesh isogeometric and the topology evolving history is depicted in Fig. 14. The topology evolving history shows that the final topology is obtained in the 69 iterations. The value of the compliance at the optimal design is 18.222.

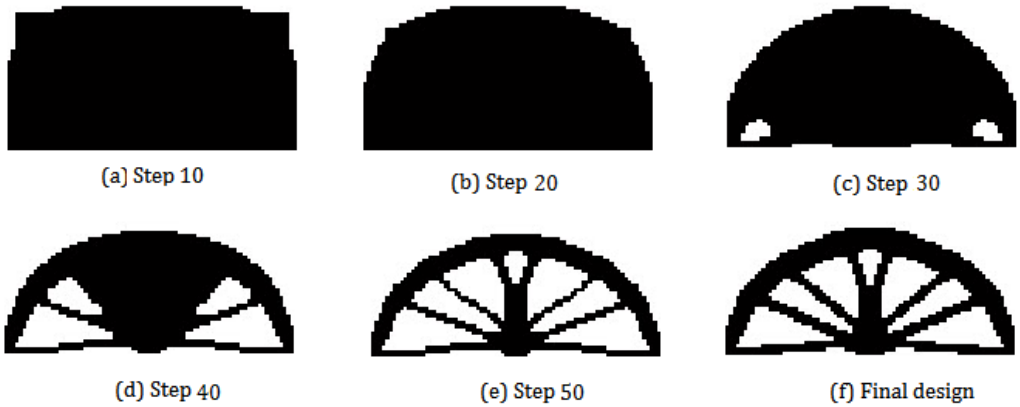

Figure 14. The evolution of optimal topology of the Michell beam

In second stage, the final topology of the example obtained by FEM as an analyzer instead of IGA in order to demonstrate the performance of the proposed method. It is noted

that the number of degree of freedoms in FEM are also equal to those of IGA. The final topology optimization obtained the proposed method is compared with that obtained by the FEM and shown in Fig. 15.

(a) (b)

Figure 15. The comparison of the final optimal topology based on (a) FEM and (b) IGA

It can been seen from Fig. 15 that the final design obtained based on the IGA is similar to that of FEM. The optimal results obtained with the two different schemes are listed in Table 3.

Table 3: Comparison of the results obtained based on the FEA and IGA

Schemes	Objective function ($J(\Omega)$)	Number of convergence Iterations
FEM	18.398	70
IGA	18.222	56

As can be seen from Table 3, the number of convergence Iterations of the IGA is considerably lower than that of the FEM. Hence, the proposed method has more stability.

8. CONCLUSIONS

In this study, a hybrid of the LSM with sensitivity schemes and IGA has been developed for topology optimization. In this LSM, the boundary propagation with topological changes is implemented using the shape gradient. Furthermore, the topological gradient method is also incorporated into the LSM to precisely design new holes in the interior domain. In the topology optimization procedure the NURBS based–IGA approach is utilized instead of in the conventional FEM.

The validity and robustness of the hybrid of the LSM with sensitivity schemes and IGA is shown through the benchmark examples widely used in topology optimization. The final topology obtained by the proposed method are compared with outcome of topology optimization based on the LSM with FEM and other LSM techniques, and the results show similar topologies. The optimization results also demonstrate that the convergence rate of the proposed method is obviously higher than that in the LSM with FEM and other LSM techniques. Therefore, the proposed method has more stability and can be considered as a powerful topology optimization algorithm.

REFERENCES

1. Dijk NP, Maute K, Langelaar M, Keulen F. Level–set methods for structural topology optimization: a review, *Struct Multidiscip Optim* 2013; **48**: 437-72.
2. Bendsøe MP, Sigmund O. *Topology Optimization: Theory, Methods, and Applications*, Springer, Berlin, 2003.
3. Bendsoe MP, Kikuchi N. Generating optimal topologies in structural design using a homogenization method, *Comput Methods Appl Mech Eng* 1988; **71**: 97-224.
4. Rozvany GIN. *Structural Design via Optimality Criteria*, Kluwer Academic Publishers, Dordrecht, 1989.
5. Rozvany GIN, Zhou M. The COC algorithm, Part I: Cross section optimization or sizing, *Comput Methods Appl Mech Eng* 1991; **89**: 281-308.
6. Schmit LA, Farsi B. Some approximation concepts for structural synthesis, *AIAA J* 1974; **12**(5): 692-99.
7. Schmit LA, Miura H. *Approximation Concepts for Efficient Structural Synthesis*, NASA Publisher, Washington, United States, 1976.
8. Vanderplaats GN, Salajegheh E. A new approximation method for stress constraints in structural synthesis, *AIAA J* 1989; **27**(3): 352-58.
9. Svanberg K. The method of moving asymptotes–a new method for structural optimization, *Int J Numer Meth Eng* 1987; **24**: 359-73.
10. Tavakkoli SM, Hassani B, Ghasemnejad H. Isogeometric topology optimization of structures by using MMA, *Int J Optim Civ Eng* 2013; **3**: 313-26.
11. Kazemi HS, Tavakkoli SM, Naderi R. Isogeometric topology optimization of structures considering weight minimization and local stress constraints, *Int J Optim Civil Eng* 2016; **6**(2): 303-17.
12. Xie YM, Steven GP. A simple evolutionary procedure for structural optimization, *Comput Struct* 1993; **49**(5): 885-96.
13. Jakiela MJ, Chapman C, Duda J, Adewuya A, Saitou K. Continuum structural topology design with genetic algorithms, *Comput Methods Appl Mech Eng* 2000; **186**: 339-56.
14. Kaveh A, Hassani B, Shojaee S, Tavakkoli SM. Structural topology optimization using ant colony methodology, *Eng Struct* 2008; **30**(9): 2559-65.
15. Osher S, Sethian JA. Front propagating with curvature dependent speed: algorithms based on Hamilton–Jacobi formulations, *J Comput Phys* 1988; **78**: 12-49.
16. Sethian JA, Wiegmann A. Structural boundary design via level set and immersed interface methods, *J Comput Phys* 2000; **163**(2): 489-528.
17. Allaire G, Jouve F, Toader AM. Structural optimization using sensitivity analysis and a level set method, *J Comput Phys* 2004; **194**: 363-93.
18. Shojaee S, Mohamadian M, A Binary Level Set Method for Structural Topology Optimization, *Int J Optim Civil Eng* 2011; **1**(1): 73-90.
19. Shojaee S, Mohamadian M, Valizadeh N. Composition of isogeometric analysis with level set method for structural topology optimization, *Int J Optim Civil Eng* 2012; **2**(1): 47-70.
20. Shojaee S, Mohaghegh A, Haeri A. Peiecwise constant level set method based finite element analysis for structural topology optimization using phase field method, *Int J Optim Civil Eng* 2015; **5**(4): 389-407.

21. Hughes TJR, Cottrell J, Bazilevs Y. Isogeometric analysis: CAD, finite elements, NURBS, exact geometry and mesh refinement, *Comput Methods Appl Mech Eng* 2005; **194**: 4135-95.
22. Xia Q, Shi T, Liu S, Wang MY. A level set solution to the stress–based structural shape and topology optimization, *Comput Struct* 2012; **90-91**: 55-64
23. Wang M, Wang XM, Guo DM. A level set method for structural topology optimization, *Comput Methods Appl Mech Eng* 2003; **192**: 227-46.
24. Osher S, Fedkiw R. *Level Set Methods and Dynamic Implicit Surfaces*, Springer, 2002.
25. Wang XM, Wang MY, Guo DM. Structural shape and topology optimization in a level-set framework of region representation, *Struct Multidiscip Optim* 2004, **27**(1–2), 1-19.
26. Sokolowski J, Zochowski A. On the topological gradient in shape optimization, *SIAM J Cont Optim* 199, **37**: 1251-72.
27. Burger M, Hackl B, Ring W. Incorporating topological gradients into level set methods, *J Comput Phys* 2004; **194**: 344-62.
28. He L, Kao C, Osher S. Incorporating topological gradients into shape gradient based level set methods, *J Comput Phys* 2007; **225**: 891-909.
29. Piegl L, Tiller W. *The NURBS Book*, Springer, 2nd edition, Germany, 1995.
30. Shojaee S, Mohammadian M. Structural topology optimization using an enhanced level set method, *Scientia Iranica A* 2012, **19**(5): 1157-67.
31. Mohammadian M, Shojaee S, Binary level set method for structural topology optimization with MBO type of projection, *Int J Numer Meth Eng* 2012; **89**(5): 658-70.